

FINAL PUBLISHABLE REPORT

Grant Agreement number 15SIB04
 Project short name QuADC
 Project full title Waveform metrology based on spectrally pure Josephson voltages

Project start date and duration:		01 June 2016, 36 months
Coordinator: Ralf Behr, PTB Tel: +49 531 592 2630		E-mail: ralf.behr@ptb.de
Project website address: https://www.ptb.de/empir/quadc-home.html		
Internal Funded Partners:	External Funded Partners:	Unfunded Partners:
1. PTB, Germany	11. APPLICOS, Netherlands	16. METAS, Switzerland
2. CEM, Spain	12. esz, Germany	
3. CMI, Czech Republic	13. USN, Norway	
4. INRIM, Italy	14. INTI, Argentina	
5. JV, Norway	15. SC, United Kingdom	
6. NPL, United Kingdom		
7. RISE, Sweden		
8. TUBITAK, Turkey		
9. VSL, Netherlands		
10. VTT, Finland		

TABLE OF CONTENTS

1.	Overview	3
2.	Need.....	3
3.	Objectives	3
4.	Results	4
4.1	Objective 1	4
4.2	Objective 2	7
4.3	Objective 3	11
4.4	Objective 4	16
5.	Impact	21
6.	List of publications	22
7.	Contact details	23

1. Overview

This project has developed measurement systems needed for fast metrology-grade waveform analysis. The new systems are centred on true alternating current (AC) voltage quantum devices which will operate at the highest level of accuracy and be simple enough for exploitation outside of the National Metrology Institutes (NMIs) community. The term 'true AC voltage quantum devices' refers to the recently achieved breakthrough which has provided spectrally pure quantised Josephson AC voltages exceeding, for the first time, the usability threshold of 1 V root mean square (RMS). This project focused on the development of a real-time quantum voltage digitiser based on optical driven Josephson junctions and 20 MHz feedback loop. Wide band voltage dividers with improved uncertainties were built to link voltages up to 1000 V to such quantum standards for frequencies up to 100 kHz.

2. Need

The need for the development of measurement systems based on true AC voltage quantum devices (or Josephson devices) was driven by their fields of application, as sensing and measurement are increasingly dependent on fast analogue to digital conversion (ADC). Recent Research & Development (R&D) in precision integrated circuits and measurement equipment has also brought about a step change increase in the sampling rates and accuracies available. Although the direct traceability of direct current (DC) electrical metrology using quantum standards is well established, there is also a need to meet the new demand of emerging measurement applications using high-end equipment which currently cannot be met by existing electrical metrology approaches

3. Objectives

The overall objective of this project was to provide direct, efficient and highly accurate traceability of AC voltages, for end-users. The specific objectives of the project were:

1. To develop a quantum-based real-time measurement system utilising the Josephson effect representation of the SI volt. Novel methods for biasing Josephson junctions, such as the use of optoelectronic devices, will be exploited to achieve larger voltage levels, as well as approaches for direct ADC in terms of the Josephson constant $K_J = 2e/h$. Specialised electronic circuits required for interfacing the sensitive and accurate low temperature Josephson devices to room temperature industrial precision waveform instruments will be developed over the range of voltages and frequencies relevant in precision waveform metrology.
2. To develop a robust and end-user friendly quantum system as a practical realisation for providing direct traceability of the redefined base unit 'volt' to end users, either national measurement laboratories or the next tier users in the calibration and test sectors. This includes automation techniques, He-free cryogenic systems (4 K) and cost-effective components.
3. To evaluate digital signal processing techniques with respect to their contribution to measurement uncertainty and to validate measurement methods for AC voltage calibration based on spectrally pure Josephson-AC-voltage references. The target uncertainty is 10 nV/V-level for frequencies up to 1 kHz and better than 10 μ V/V up to 1 MHz. This will be validated via calibration of commercial instruments against a quantum standard and performed in collaboration with manufactures of precision instrumentation.
4. To scale quantum waveforms up to 1 kV using voltage dividers or amplifiers. By measuring the divider output directly with a Josephson based digitising system the higher voltage waveform will be linked to the Josephson volt; the ultimate aim is to reach uncertainties ranging from 5 μ V/V at 1 kV / 50 Hz to 25 μ V/V at 120 V / 100 kHz.
5. To engage companies in the project research to facilitate the take up of the technology and measurement infrastructure developed by the project, and to support the development of new, innovative products, thereby enhancing the competitiveness of EU industry.

4. Results

This section gives an account of the project's outputs delivered against each of the project's objectives.

4.1 Objective 1

Development of a system able to make real-time measurement of arbitrary voltage waveforms, traceable to the SI volt, was required to meet Objective 1. This system is known as a quantum voltage digitiser (QVD). Prior to this project, such a system had not been demonstrated either by the consortium or elsewhere.

4.1.1 Quantum Voltage Digitiser

In this project, the hardware for a quantum voltage digitiser was designed, built, tested and integrated to form a working system. An overview of the hardware is shown in the schematic diagram in Fig.1. The arbitrary voltage waveform is input to the delta-sigma electronics. The custom analogue delta-sigma electronics (see in Fig.1.) have been designed to have a large operating bandwidth (DC to 1 MHz) and large signal to noise ratio (noise transfer function of -200 dB at kHz frequencies). The output of the analogue stages is measured by a fast analogue to digital converter (ADC) that is integrated with a field programmable gate array (FPGA) system. The FPGA controls the feedback loop which operates at around 5 MHz. It converts the input ADC reading into a pulse pattern containing 1024 pulses at a 5 GHz pulse rate, using a look up table. This pattern is sent to the optoelectronic pulse drive system. The FPGA also records and transmits the pulse pattern to a host computer where the data can be analysed using the user interface described in Deliverable 4. The optoelectronic system is based on telecoms in-fibre laser components operating at a wavelength of 1550 nm. The electrical pulse pattern is converted into the corresponding optical pulse pattern. Details of this optoelectronic pulse drive and its performance parameters have been published in Fig.2. The electrical pulse pattern is converted into the corresponding optical pulse pattern. An electrically isolated photodiode, mounted on the cryostat, is used to convert the optical drive signal back into an electrical drive to drive the Josephson junction array (JJA). In future systems the photodiode will be mounted at low temperature as developed in WP2 of this project. The JJA outputs a quantum-accurate voltage, which is precisely known from the FPGA code. This is fed back around the feedback loop to the input of the delta sigma electronics, which act to minimise the difference in the feedback and arbitrary voltage. In this way, the FPGA code represents a quantum-accurate digitisation of the input arbitrary voltage waveform. The system is described in detail in Deliverable 2

The testing of the QVD system is described in Deliverable 4. It was tested for input frequencies from dc up to

Quantum Voltage Digitiser

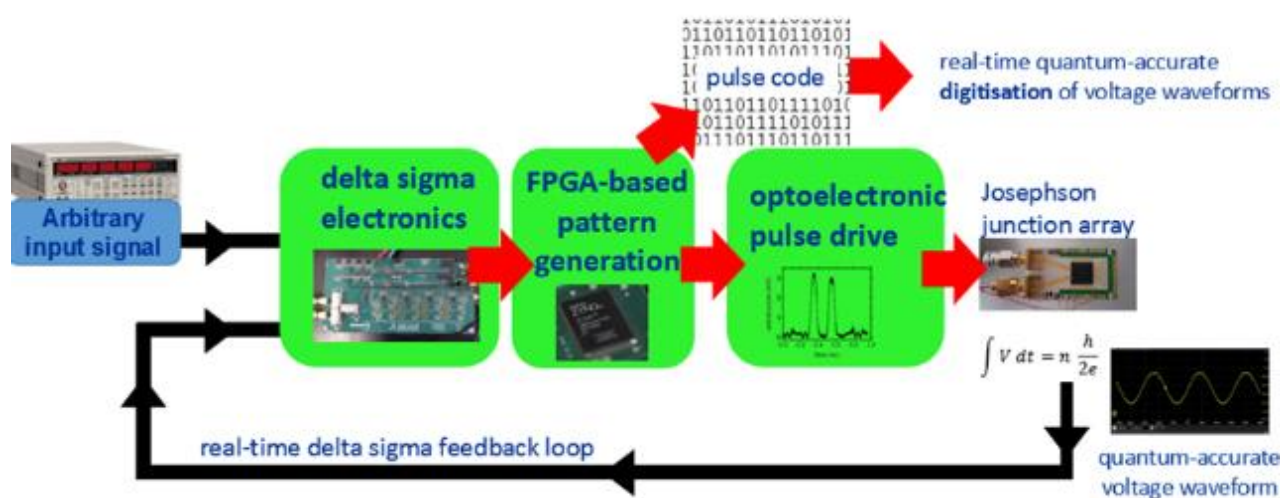


Fig.1: Schematic diagram of Quantum Voltage Digitiser

100 kHz. The QVD was found to follow the input over this range. The system will operate in principle up to 1 MHz with greatly increased uncertainties. It is fully understood that this happens due to a sharp roll off in

amplitude with increasing frequency. However, the use of the four integration stages of the delta sigma electronics (instead of the existing first stage only) will reduce uncertainties. The optimisation at the higher frequency range is the subject of future work. A typical example of a measurement is given in Fig. 2. for an input sine wave of 2 mVpp amplitude at a frequency of 8179 Hz.

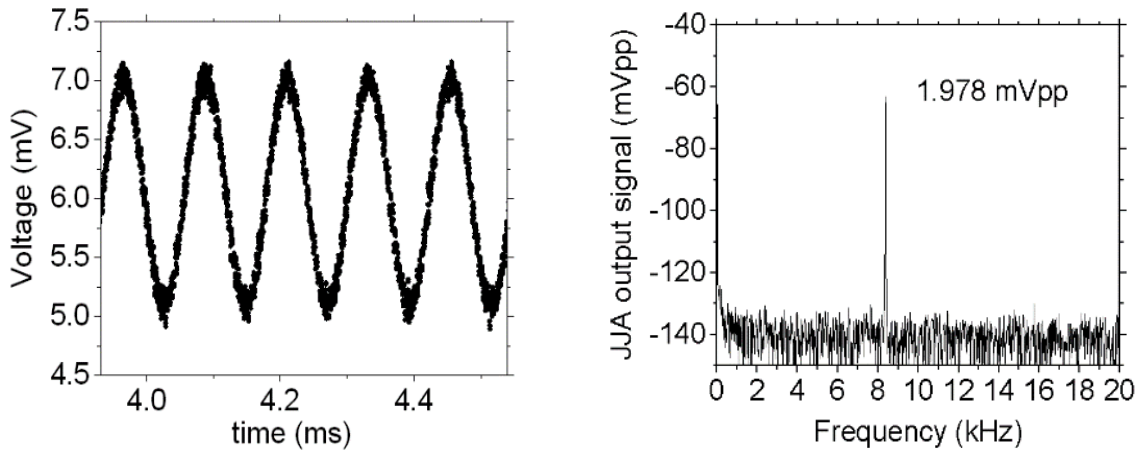


Fig.2: Typical voltage output of JJA and the corresponding FFT. The voltage is obtained by converting the look up table row pattern into a voltage.

The frequency response of the QVD was examined using a sinusoidal input from a signal generator, as shown in Fig.3. The QVD system was also used to measure the output of the PTB Josephson Arbitrary Waveform Synthesizer (JAWS) system, as described in Deliverable 1. The measured values are obtained using the software described in D4 to fit the data obtained from the QVD. This data is the record of the pulse code that

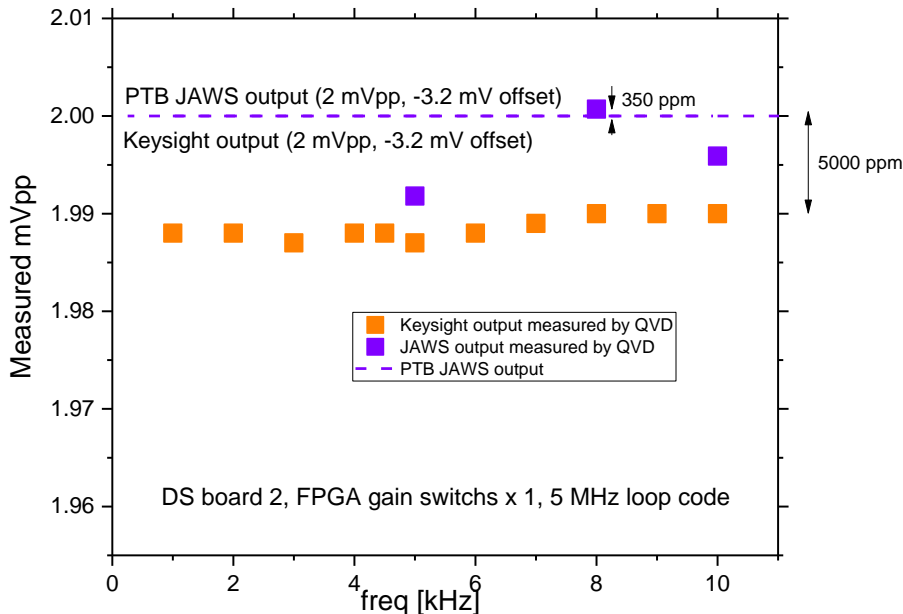


Fig.3: Measurements made using the QVD containing the delta Sigma board with higher gain (Board 2). For input sinusoidal waveforms at various frequencies, the JJA pulse pattern is recorded and converted into a voltage waveform. A fit using the software described in Deliverable 4 is performed to obtain the amplitude of the waveform which is plotted as a function of frequency. Measurements are shown of the output of a Keysight audio signal generator (orange squares) and the output of the PTB JAWS system (purple squares). The offset is due to the difference between the set value and the output value of the voltage source.

was sent to the JJA in order to match the arbitrary input waveform. From the known number of pulses per unit time and the known quantised area of the voltage-time pulse the output voltage can be calculated.

4.1.2 Photodiodes for 4 K operation

An optoelectronic module for operation at 4 K was developed, intended for use in a pulse-driven JAWS system. Multiple InP/InGaAs photodiodes with customized optical fiber assemblies were assembled on a single silicon carrier. Photodiodes were flip-chip bonded on the carrier using Au stud bumps, and laser-cut silicon fixtures were aligned and adhesively bonded to the carrier in order to attach pigtailed borosilicate ferrules (see Fig.4.). Optical simulations were performed to estimate the tolerance for fiber-chip misalignment. The photodiodes were bonded with an average misalignment of 8 μm , while the misalignment between the silicon fixture and the photodiodes after bonding was 13 μm .

The electrical response to continuous wave laser inputs was measured at room temperature and at 4 K by direct immersion in liquid helium. The results show that the assembly technique could facilitate a stable and efficient optical coupling. The individual photodiodes were able to deliver currents up to 12 mA at room temperature and 7 mA at 4 K.

A Mach-Zehnder modulated laser was fibre coupled to the photodiode at 4 K and produced electrical pulses with pulse peak heights in the range 10-16 mA for full-width-half-maximum down to 77 ps. At 10 GHz clock frequency, at a 25 % duty-cycle, the waveform has been demonstrated to be stable over the time span of 90 minutes. Measured waveform data has been used to perform simulations, based on the Stewart-McCumber model, of the flux-quanta transport through a typical Josephson junction.

In addition, the high-speed pulsation of two cryogenically-operable, bipolar photodiode module prototypes have been made. Versions with and without 50 Ω on-chip termination of the high-frequency transmission lines on the photodiode chip-carrier have been manufactured and tested in liquid helium. Both a Mach-Zehnder-modulated continuous-wave laser and a fast mode-locked laser have been used as source of fast laser pulses.

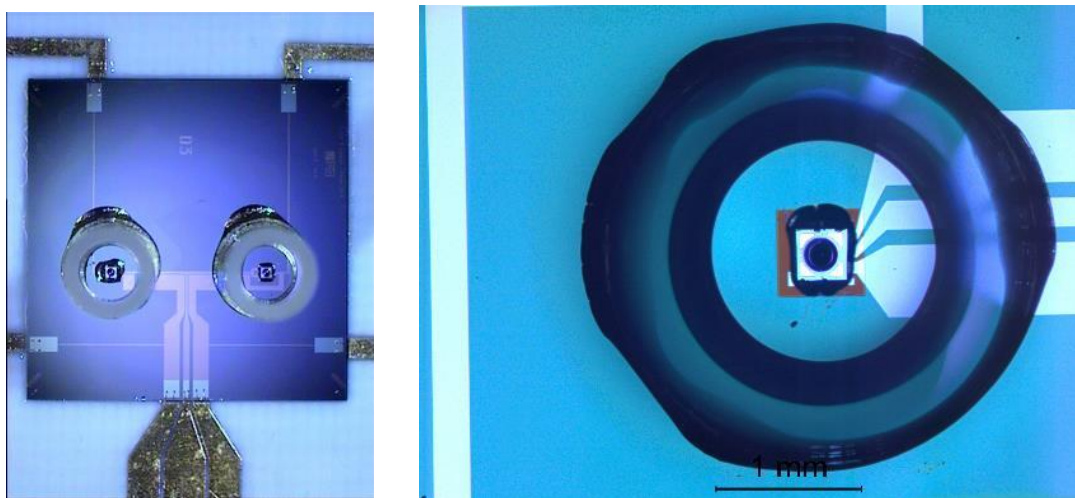


Fig. 4: Left image - Photograph of chip-carrier on the bipolar photodiode module. The picture shows the photodiodes centered inside the borosilicate glass sleeves, through which the optical connection will be made using ferrule-ended optical fibers. Right image - Close-up picture of the photodiode through the glass sleeve. The photodiode is the lensed bottom-illuminated version of the PD20X1 from Albis.

Photo-current pulses with peak height up to 6.34 mA, and full-width-at-half-maximum down to about 37 ps have been measured. A model of the prototypes has been constructed in COMSOL Multiphysics, which has been verified by measured pulse waveforms. In order to reduce the reflective behaviour in future designs, the model has been used to suggest an improved design of the bipolar photodiode module, by placing the positively and the negatively coupled photodiodes closer to each other, reducing the center-to-center separation from 4.5 mm to 500 μm .

Modulation of the continuous pulse train from the mode-locked laser into simple bit patterns has been performed using a Mach-Zehnder modulator to select pulses to be transmitted to the photodiodes. Simultaneous bipolar operation of a bipolar module has also been demonstrated (see Fig. 5).

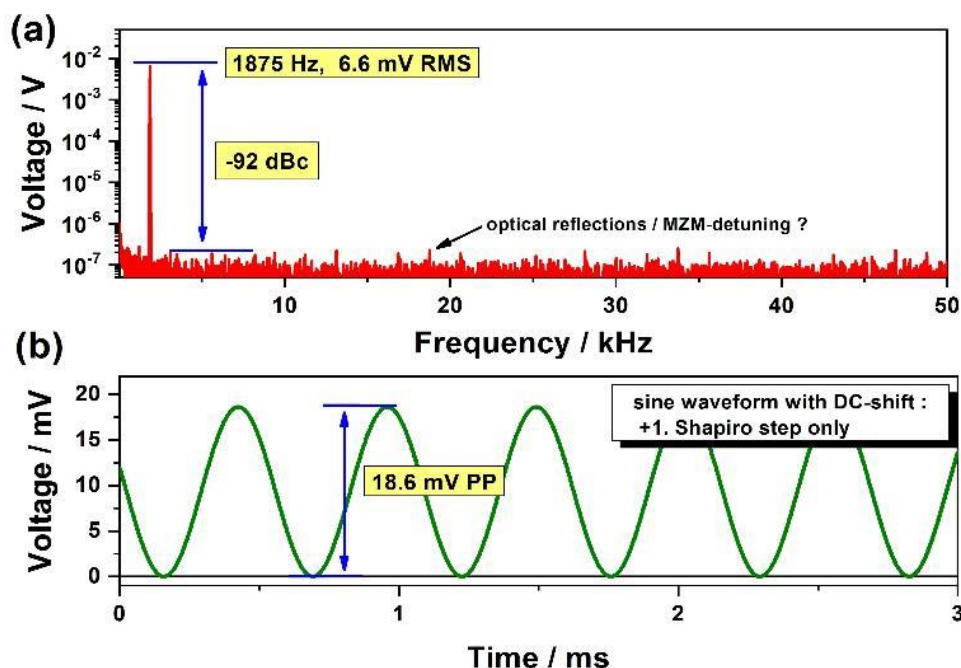


Fig. 5. (a) Frequency-spectra and (b) time-domain of a unipolar sinusoidal waveform at a signal frequency of 1875 Hz and amplitude of 6.6 mV RMS. A PD operated at 4 K and 15 GHz was used to provide the pulses to the JAWS array with 3000 junctions.

In summary, the digitisation of voltage waveforms using the real-time feedback loop has been demonstrated. This represents the development of new capability in quantum voltage waveform metrology. The system is capable of operation up to the MHz frequency range.

The technology of mounting photodiodes has greatly improved and developed into a reliable procedure during the project. Further work has been started towards a bipolar assembly of the photo diodes. Objective 1 has therefore been met.

4.2 Objective 2

The QVD system described above was developed using mostly commercially available hardware. Off-the-shelf electronic components (ADCs, FPGA) and telecoms optical components were used. This allows the final system cost to be reduced. In particular, the use of an FPGA replaces the requirement for an expensive electrical pulse pattern generator (PPG). The use of an optoelectronic drive offers a future lower cost way of scaling to larger voltages. It uses common low-cost optoelectronic components to provide multiple drive channels. The electrical alternative requires electrical PPGs and complex compensation electronics that requires specialist adjustment by a trained operator. In addition, the QVD system has been integrated with user friendly software. This provides comprehensive facilities for data analysis. In summary, the QVD hardware has been designed such that it is suitable for widespread use in metrology and calibration labs and so that further upgrades can be performed in the future.

4.2.1 Cost-effective optical pulse pattern generator for driving Josephson junction arrays

Josephson arbitrary waveforms synthesizers are expected to continue developing in a direction whereby current pulses driving the Josephson junction arrays (JJA) are generated with optical pulses fed to nearby ultra-fast photodiodes. An obvious way to generate fast optical pulses for this purpose is to use a continuous-wave laser and optical intensity modulators to shape the pulses (approach selected by NPL, for example). Typically, very expensive electronic pulse pattern generators operating at tens of GHz frequency are used to drive the modulators. In this project, VTT proposed a novel concept potentially providing technical advantages as well as addressing the cost problem. VTT investigated an idea to build an optical PPG utilizing a pulsed laser as the core part of the source and generating the targeted pulse pattern by passing selected pulses while blocking the others using intensity modulators (pulse picking). During the project, VTT designed and built an

optical PPG and tested the main components with JJAs. This section gives an overview of the work and main results and more details will be published soon (see Fig.6.)

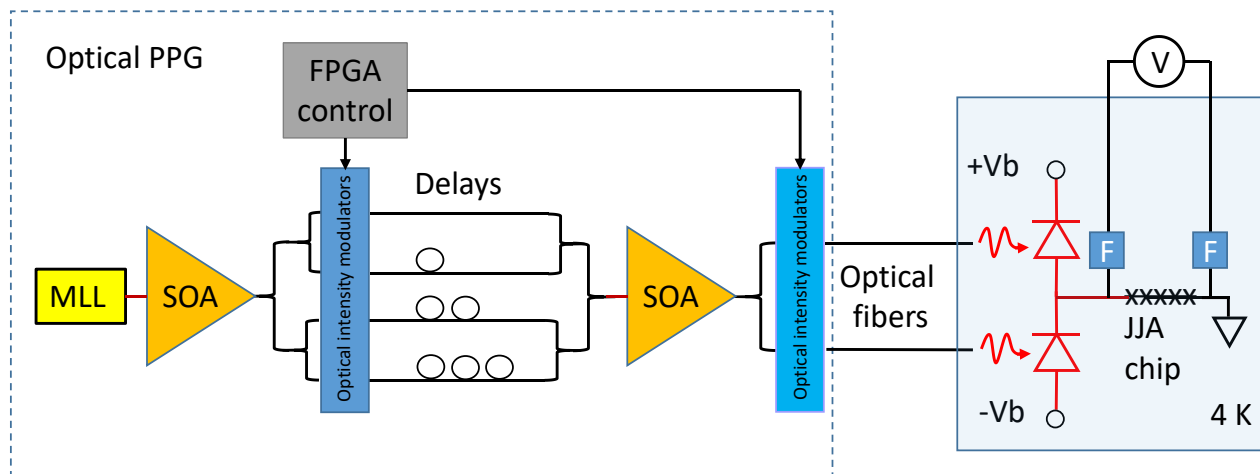


Fig. 6: A simplified diagram of a quantum ac voltage standard which is the ultimate overall goal of this research. The standard is based on an optical pulse pattern generator with a pulsed laser and cryogenic photo diodes. The key part of the PPG is a custom-made mode-locked laser (MLL). SOA stands for a Semiconducting optical amplifier and FPGA for a Field-programmable gate array (evaluation board). The fiber optic splitters and delay lines form an optical time-division multiplexer used to multiply the MLL pulse rate (by a factor of four in this illustration). The on-chip filters (F) attenuate the high-frequency noise resulting from the driving pulses.

Fig. 6. shows a simplified illustration of a quantum ac voltage standard where an optical PPG based on a pulsed laser acts as a pulse source. The PPG feeds optical pulses to two photo diodes at 4 K via two optical fibres. The photo diodes are biased electrically such that they provide current pulses in both polarities to the JJA chip as required. This allows realization of truly bipolar output voltage waveforms with the JJA. The main components of the optical PPG built by VTT are a mode-locked laser (MLL), semiconducting optical amplifiers (SOA), optical fibre splitters, optical intensity modulators (OIM), optical delay lines, and control electronics for driving the OIMs. A key part of the control electronics is a field-programmable gate array (FPGA) evaluation board. The digital pulse pattern is uploaded into the memory of the control electronics via a personal computer (PC) before starting the transmission of the pulse pattern (generating the JJA output waveform).

Mode-locked lasers (MLL) are devices which typically produce pulse trains with little amplitude variation and time jitter. With the added capability to produce very fast pulses (down to the ps range) they seem to offer an ideal solution for producing pulses for JJAs even at higher rates than targeted in QuADC. VTT designed and built several versions of an MLL using commercially available optical components. The pulse rate of the latest version of the MLL is variable in the range of 2-2.5 GHz, width of the pulses is 10-15 ps (half width), the wavelength is 1340 nm and the peak power is 15 dBm.

One of the main design points of the PPG, both from the technical performance and cost point of view, is that the MLL operates only at a relatively moderate frequency, typically 2-2.5 GHz. The seed pulses generated by the MLL are fed to the rest of the PPG which essentially composes a time-division multiplexer (TDM) with integrated pulse picking system. The TDM increases the pulse rate such that sufficiently high voltages are obtained from the JJA. For example, using the TDM with four channels (see Fig.6.), and an MLL pulse rate of 2.5 GHz, results in an output pulse rate of 10 GHz. In principle, the pulse rate can be increased by increasing the number of channels in the TDM. In practice, the pulse rate is currently limited by the speed of the available photodiodes to approximately 20 GHz.

Two examples of pulse trains generated with the optical PPG built by VTT are shown in Fig. 7. left (unmodulated) and right (modulated). This data was recorded using a room-temperature photodiode (20 GHz bandwidth) and a 20 GHz oscilloscope. It seems that the properties of the optical pulses are preserved when passing through the pulse picking system and sufficient attenuation of unwanted pulses is obtained. Some ringing immediately after the pulse is observed, arising probably both from the photodiode and the measurement circuitry. This may have some minor negative influence on the standard performance at highest pulse rates although likely not significant.

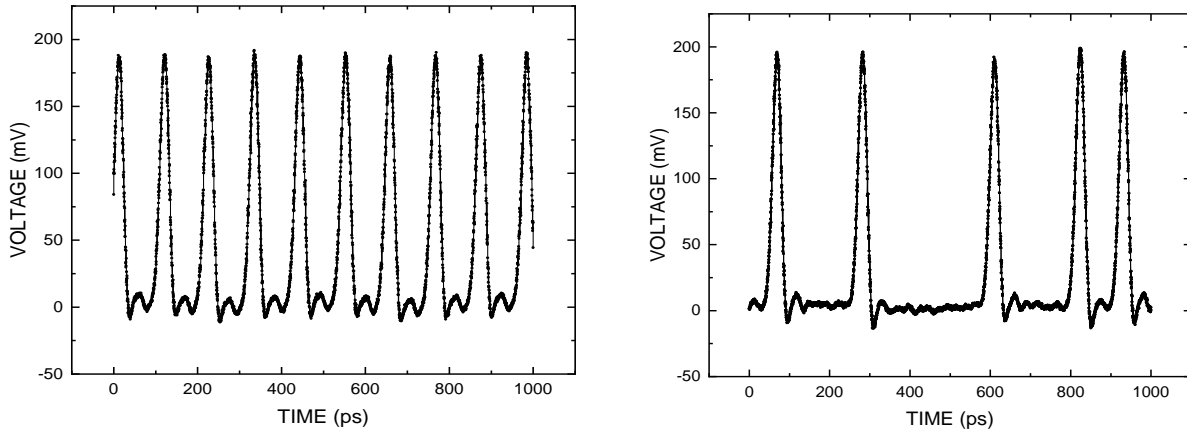


Fig. 7: Left image - Pulse stream through the time-division multiplexer of the PPG, and optical amplifier at the end. In this example the pulse rate is $4 \times 2.3 \text{ GHz} = 9.2 \text{ GHz}$. Right image - An example of a modulated pulse stream (101001011...).

The suitability of a custom-made MLL to drive JJAs has been tested extensively during the project. Several optical configurations were designed and built to solve various problems, related mostly to the stability of outgoing pulses. At the end of the project VTT has built an MLL which allows quantized voltage waveforms to be generated. Fig. 7. shows a demonstration that an MLL is capable of generating pulses which can be used to drive a JJA successfully. An unmodulated even current pulse train using a room-temperature photodiode was fed through the JJA and output voltage measured as a function of so-called compensating dc current. Voltage plateaus are observed both at a pulse rate of 2.2 GHz and 8.8 GHz (see Fig. 8.) shows a magnified view of the plateau measured at 2.2 GHz illustrating good degree of quantization.

First experiments with a photodiode in the liquid helium bath next to the JJA were also carried out. The early results were very promising, but unfortunately measurements were interrupted by early breakage of the photodiode. This failure was however probably due to excess optical power delivered to the component (human error). Collaboration with HSN has agreed the delivery of new photodiodes and experiments at VTT will be continued soon after the project with internal funding. Furthermore, experiments to investigate the performance of the full PPG apparatus in producing time-varying pulse patterns are to be carried out.

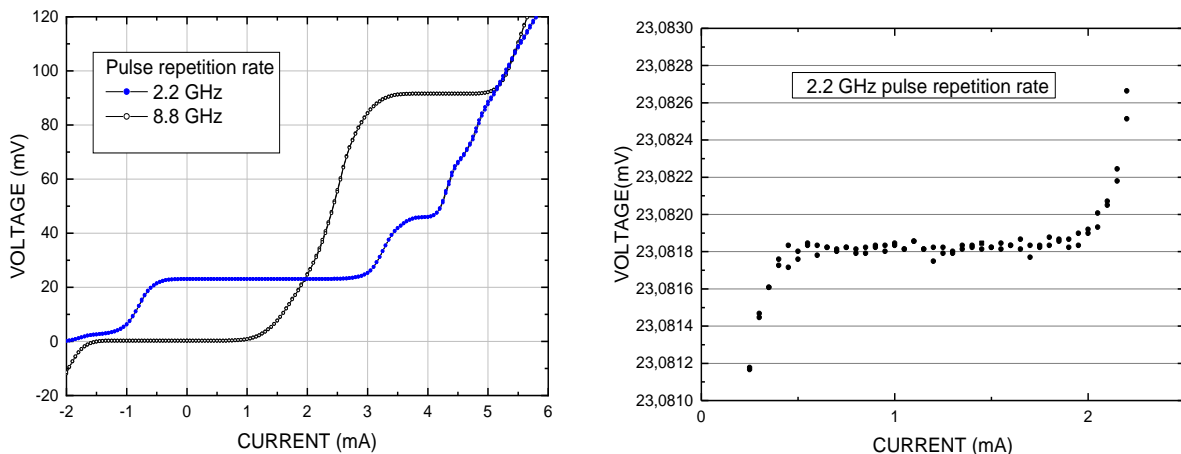


Fig. 8: Left Image - Josephson junction array voltage as a function of the dc compensating current at current pulse rates 2.2 GHz and 8.8 GHz. The current pulse amplitudes were set for widest possible plateaus. Right) Magnified view of the data measured at 2.2 GHz shown in left panel.

The proof-of-concept prototypes of an optical PPG built so far were all based on bulky commercially available optical components. In VTT's vision, there is plenty of room in reducing the overall cost and improving the technical performance by proper integration techniques. This work has already been granted further funding

at VTT. This should allow more affordable PPGs to come to marketplace and thereby enable wider adaptation of quantum standards for time-varying voltage waveforms by national metrology institutes.

4.2.2 Test of short cable correction with a cryocooler

The interest to increase the speed of signals motivates the quest for a quantum voltage standard operating at higher frequencies and for the generation of quantum accurate arbitrary signals with very low-rise times. At present, pulsed standards are most promising for that, however there are limitations in increasing the operating speed, mainly due to the capacitive loading of the array. The main contribution to loading is to be found in the cables that connect the array in the cryogenic environment to the measurement setup. The shortened connections in cryocooled standards seem then interesting to mitigate this unwanted effect.

To estimate the possible benefits of the reduced length of cables in a cryocooled JAWS, INRIM measured the residual difference to quantum generated ac and dc signals by means of a thermal transfer standard (see Fig. 9.). First results showed a dependence on frequency that is likely to be related to a non-quantized condition of the array, probably due to capacitive currents through cable parasitic effects. Methods to detect and correct for non-quantized working conditions are currently studied.

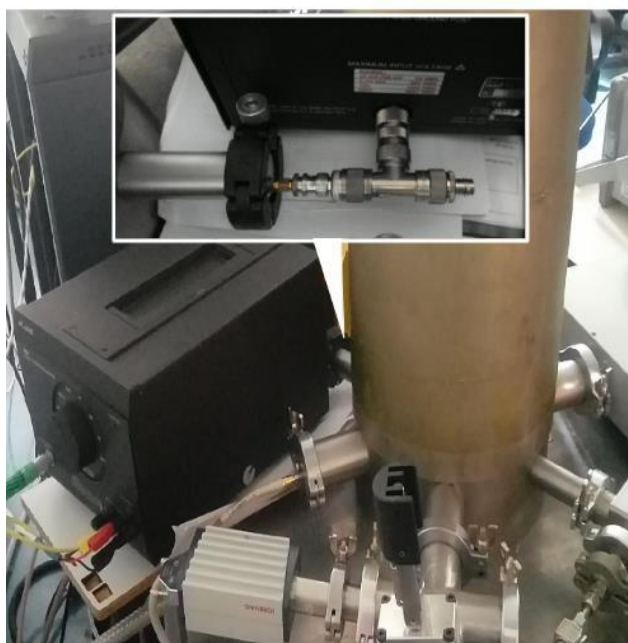


Fig. 9: Straight connection from cryocooler and ac/dc thermal transfer standard.

4.2.3 User friendly software

A robust and user-friendly software integrating automation techniques and algorithms for use and application of the new quantum AC voltage standard has been developed. The presented software is based on several parts:

1. Quatsch calibrator – system to automatize the whole calibration of a calibrator. One can download it here: https://gitlab.com/KaeroDot/quatsch_calibrator
2. Quatsch driver – driver for the FPGA used in the quantum AC voltage standard. The driver itself is accessible at GitLab: https://gitlab.com/KaeroDot/Quatsch_driver
3. TWM – TracePQM Watt Meter, front end connecting drivers and QWTB. It can be downloaded here: <https://github.com/smaslan/TWM>
4. QWTB – QuWave ToolBox, toolbox of various algorithms. It can be downloaded here: <https://qwtb.github.io/qwtb/>
5. GOLPI – GNU Octave LabVIEW Pipes Interface, interface between LabVIEW and GNU Octave used to calculate results by means of algorithms in QWTB. It can be downloaded here: <https://github.com/KaeroDot/GOLPI>

6. GNU Octave or Matlab – one of these programming environments for scientific computing is required to run calculations:

<https://www.gnu.org/software/octave/>

<https://www.mathworks.com/products/matlab.html>

All these parts are required to run the whole software however, all parts are open access and can be downloaded from the internet. The flow of the software is shown in Fig.10. This software builds on the results of following previous EMPIR projects: Q-Wave, ACQ-PRO and TracePQM.

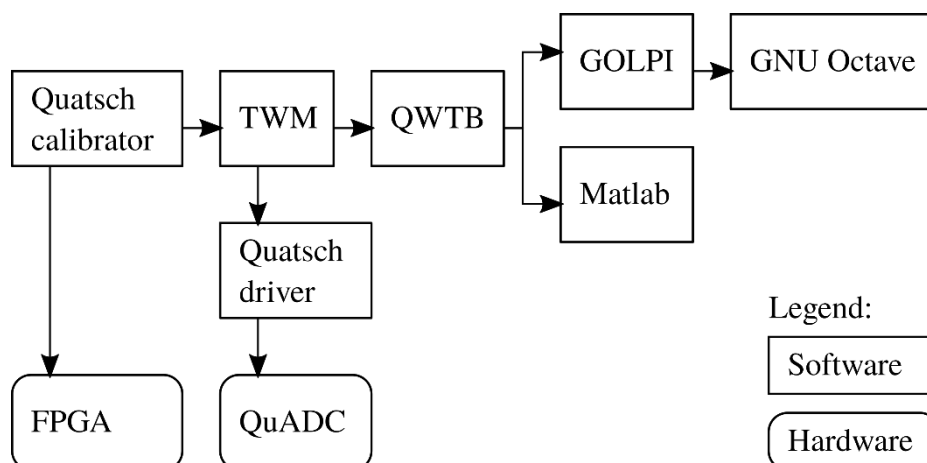


Fig.10: Flow-chart of the user-friendly software and hardware.

In summary, proof-of-concept prototypes for parts of an optical PPG have successfully been tested. So far, they all were built on bulky commercially available optical components. In VTT's vision, there is plenty of room in reducing the overall cost and improving the technical performance by proper integration techniques. This should allow more affordable PPGs to come to marketplace and thereby enable wider adaptation of quantum standards for time-varying voltage waveforms by national metrology institutes.

User-friendly software has been developed by CMI and was successfully tested during an on-site comparison between the Josephson Arbitrary Waveform Synthesizer (JAWS) and the Quantum Voltage Digitiser. This software is freely available for everybody.

Mounting of JAWS arrays into Helium (He)-free cryogenic systems (operating at 4 K) has been investigated, as well as, ways to integrate an optical drive with photodiodes. Overall, Objective 2 has been met.

4.3 Objective 3

The project worked in many ways to evaluate digital signal processing techniques with respect to their contribution to measurement uncertainty and to validate measurement methods for AC voltage calibration based on spectrally pure Josephson-AC-voltage references. Different methods to bring the quantum accurate waveforms from the chip at 4 K to devices at room temperature without deviations have been investigated. Furthermore, quantum standards have been validated via calibration of commercial instruments and in collaboration with manufactures of precision instrumentation.

The Josephson arbitrary waveform synthesizer is a perfect digital-to-analogue converter that produce quantum-accurate distortion-free voltage waveforms over frequencies between a few Hz and 1 MHz. However, the voltage leads to the DUT cause the output voltage to show deviations that quadratically scale with the frequency. These frequency dependent deviations turn out to be the dominant source of uncertainty for frequencies above approximately 10 kHz.

The original approach undertaken at METAS to suppress this quadratic frequency dependence is to develop a setup that cancels the loading effect due to the cable and decreases the difference between the voltage applied to the DUT and the calculated voltage at the Josephson junction array (see Fig. 11.).

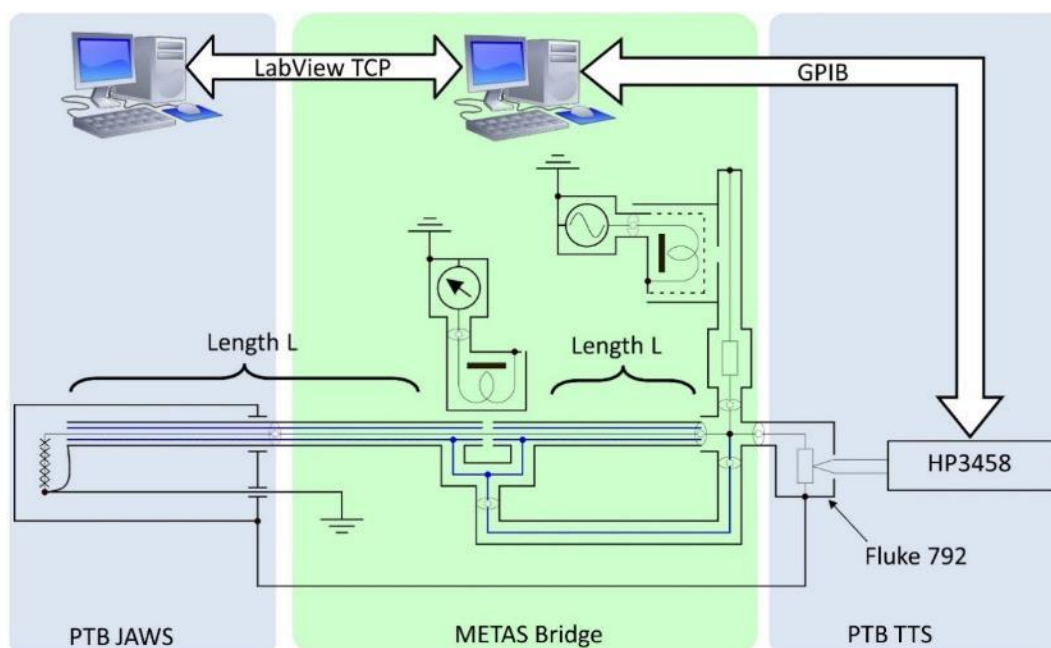


Fig. 11: Experimental set up showing the load compensation bridge connected to the JAWS. The output voltage of the LCB is read by a freshly calibrated Fluke 792 thermal transfer standard coupled to a high-end digital multi-meter.

The load compensation bridge (LCB) was tested for the first time during a measurement campaign performed at PTB during March 2019. Using an active guard to compensate the capacitive current drawn by the system wiring, the quadratic frequency dependence present at the output terminal of the JAWS was completely eliminated (see Fig.12.). Presently the uncertainty of the load compensation bridge is around a few $\mu\text{V}/\text{V}$ for voltages around 100mV and frequencies up to 80 kHz. This original result represents a real breakthrough in the voltage metrology area.

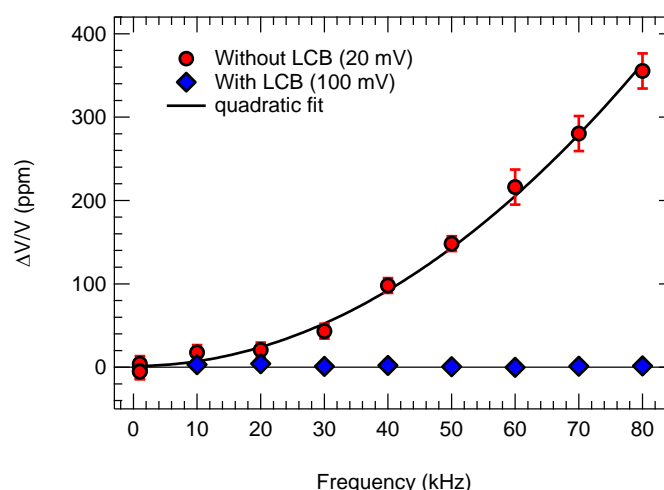


Fig. 12: Voltage measured at the output of the Fluke 792A thermal transfer standard (TTS), normalized at 1 kHz, as a function of the frequency. The red curve was measured at 20 mV without injecting any compensation current with the LCB. A clear quadratic frequency dependence is observed. The blue curve was measured at 100 mV after the LCB is fully balanced. The frequency dependence has completely disappeared up to 80 kHz.

4.3.1 Impedance matching – Simulations

A pulse-driven AC Josephson Voltage Standard generates calculable AC voltage signals at low temperatures, whereas measurements are performed at room temperature. The voltage leads cause the output voltage to show significant deviations that scale with the frequency squared. Error correction mechanisms investigated

so far allow the ACJVS to be operational for frequencies up to 100 kHz. The original method developed by VSL is based on applying a correction term proportional to the frequency squared with a proportionality constant such that at the reference point, for example at 1 MHz, the deviation is fully canceled, and the uncertainty is that of the TTS at that point, whereas at lower frequencies the uncertainty of the correction scales down with the frequency squared.

In this project, two new approaches have been chosen to increase the frequency range of the error corrections: a load compensation bridge developed by METAS, based on detecting and re-injecting the current in the voltage leads, and an impedance matching technique developed by VSL, based on prevention of reflection of electromagnetic waves.

Impedance matching at the source side of the system in liquid helium, which is loaded at room temperature with a high-impedance device under test such as a Fluke 792A thermal transfer standard, has been proposed as an accurate method to mitigate voltage lead errors for frequencies up to 1 MHz. Simulations showed that the influence of non-ideal component characteristics, such as the tolerance of the matching resistor, the capacitance of the load input impedance, losses in the voltage leads, non-homogeneity in the voltage leads, a non-ideal on-chip connection and inductors between Josephson junction array and the voltage leads, can be corrected for using the proposed procedures.

However, the procedure is quite complicated and consists of several steps:

1. inserting a resistor $R \approx Z_0$ at 4 K such that adding an extra cable does not change the output reading anymore and measure the frequency response,
2. adding a resistor $(\sqrt{2}-1) \cdot R$ at room temperature and measure the frequency response again,
3. calculate the voltage V from the ratio of steps 1 and 2 - uncertainty of $6 \mu\text{V/V}$ at 100 kHz can be obtained,
4. results can be improved using an even more complicated procedure, such that an expanded uncertainty of 12 parts in 10^6 at 1 MHz and 0.5 part in 10^6 at 100 kHz is within reach.

Apart from the complexity of the procedure, it is very difficult to experimentally prove that the assumptions can be met and that the corrections used are correct. Therefore, a simplified method is proposed, which is a combination of the above-mentioned procedure and the original correction method proposed in [10]. This combined approach makes use of the fact that the first step of the complex impedance matching procedure, which is to apply a series resistance of 50Ω at the chip, already suppresses the quadratic-frequency error, just as when using a very short cryoprobe.

To verify the quadratic-frequency response after inserting a 50Ω at the chip, simulations have been performed using the schematic described in. This schematic includes the Josephson array as an ideal voltage source, the on-chip inductance and on-chip non- $50\text{-}\Omega$ voltage leads, the matching resistor, a lossy $50\text{-}\Omega$ transmission line between 4 K and room temperature, and the input resistance and capacitance of the load.

For a TTS with $10 \text{ M}\Omega$ input resistance, an on-chip inductance of 125 nH , $3 \text{ cm } 100\text{-}\Omega$ voltage leads and $1.5 \text{ meter } 50\text{-}\Omega$ cable, for input capacitance values between 40 pF (as for the Fluke 792A) and 500 pF , the error (expressed as an AC-DC difference) is shown in the figures on the right and below (Fig. 13 and 14). As can be seen for this specific situation, between 170 pF and 180 pF the error changes sign, but the absolute value of the error still scales with the frequency squared. The deviations from this behavior show up at the lowest frequencies and seem to be less than 1 nV/V only. Changing the input resistance to $1 \text{ M}\Omega$ did not change this conclusion.

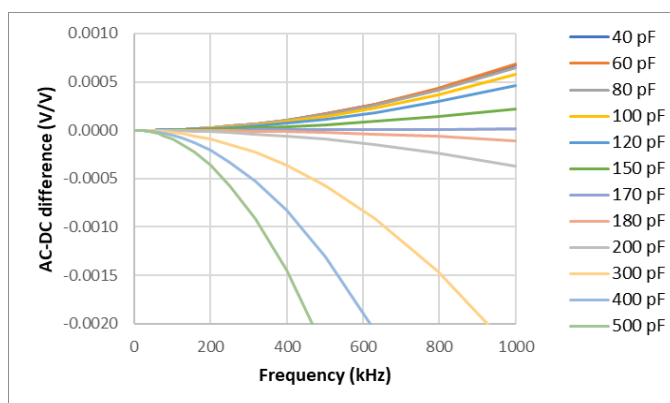


Fig. 13: AC-DC difference simulation as function of frequency and input capacitance.

Next, the effect of the mismatch between the inserted resistor and the characteristic impedance of the voltage leads was investigated. For an input impedance of $10 \text{ M}\Omega$ with 170 pF in parallel, the inserted resistance value was changed from the original 0Ω to 45Ω , 50Ω and 55Ω , for voltage leads with $50\text{-}\Omega$ characteristic

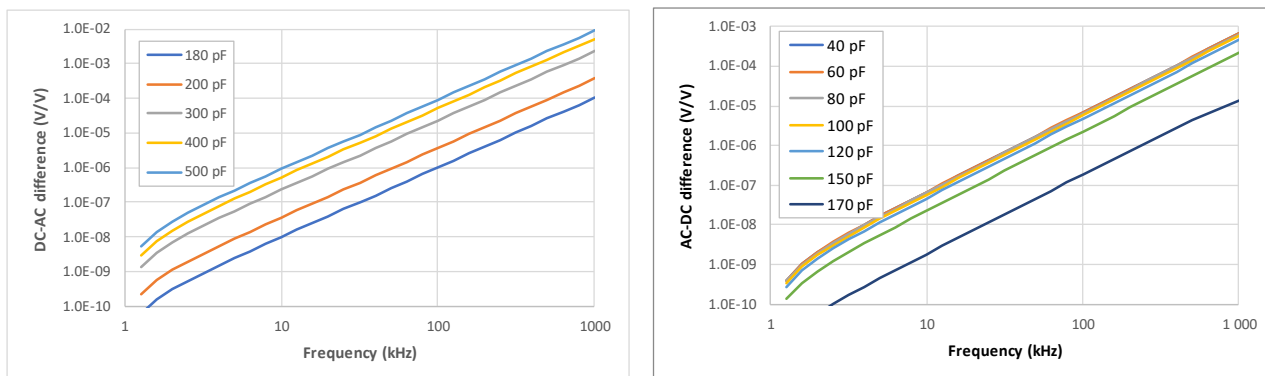


Fig. 14: AC-DC simulation as function of frequency for different parameters – see text.

impedance. The behavior was still found to be quadratic in frequency over the whole frequency range for AC-DC difference values above 10 nV/V. As a last test, the characteristic impedance of the wires connecting the inserted 50-Ω resistor to the array was varied from 50 Ω to 100 Ω and 150 Ω. Also, in this case the error was still quadratic.

In conclusion, the simulation results described above show that inserting a 50-Ω resistor close to the Josephson chip reduces the error significantly, i.e., by a factor of 10 to 100. Hence, this much simpler method is suitable for combination with the original method of correcting for the squared frequency error.

4.3.2 Impedance matching – Experimental demonstration

To demonstrate this method experimentally, we first measured the characteristic impedance of the voltage leads using a Vector network analyzer. For both the twisted pair cables and the semirigid coaxial cable the impedance was close to 50 Ω, though the semirigid cable showed characteristics closer to 50 Ω with less deviation along the frequency scale. For this reason, we changed the voltage leads to a semirigid cable.

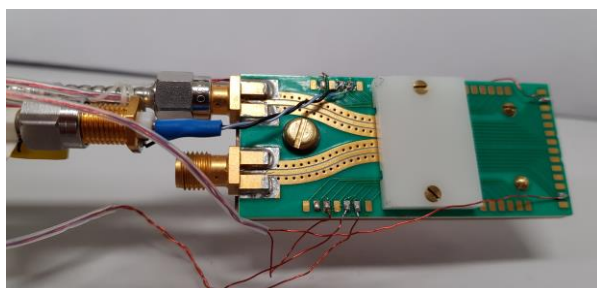


Fig. 15: Picture of the Josephson array on the sample holder and twisted-pair connections.

Next, we selected an SMD-type 50-Ω resistor and tested its temperature dependence. The resistance value changed by no more than 0.05 % when immersed in liquid nitrogen. This resistor was connected to the inner of an SMA connector piece. The resulting construction was connected to the semirigid cable and to the array by means of a short twisted-pair cable, as shown in the photograph on the left by insulation (blue tube in Fig. 15). The semirigid cable is the one used to drive the second array on the chip with pulses. We decoupled this semirigid cable and used only the other, single array.

To avoid ground loops and other experimental problems, we used the array at 20 mV only, for which we did not need to use the LF compensation. Unfortunately, the results did not show the expected suppression of the error, as can be seen in the figure on the right. In Fig. 16, the results with and without a matching resistor are shown. As can be seen, around 700 kHz an unexpected behavior was observed. Until now, we have not been able to explain this behavior and apply the necessary changes to the system to avoid this behavior.

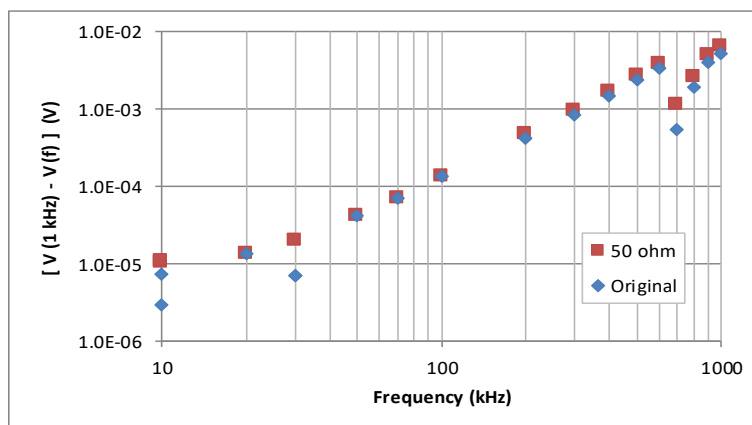


Fig. 16: Results with and without matching resistor.

New simulation results indicate that the insertion of a 50-Ω resistor suppresses the error caused by the voltage leads but keeps the quadratic frequency dependence. In combination with other suppression techniques, such as using a shorter probe, this opens the route to using the ACJVS with uncertainties below on the order of 1 μV/V at frequencies until 100 kHz. Unfortunately, a good experimental demonstration is still lacking.

4.3.3 Calibration of commercial instruments

Within the QuADC project signal generators from three stakeholders have been used as transfer standards. These were a Calibrator 5720A from Fluke, an AWG 1104 from Active Technologies, and a DualDAC 3 from Aivon Oy. First the devices have been calibrated at PTB Braunschweig using an AC quantum voltmeter. Then the generators have been transferred to the esz AG in Eichenau by car, and three days later back to Braunschweig. All synthesizers were easy to operate, and measurements ran smoothly.

This on-site comparison demonstrates that transfer standards such as Fluke 5720A calibrator or Aivon DualDAC3 are suitable for such comparison at μV/V-uncertainty level (see Fig. 17.). Improvements are possible for the DualDAC3 when having better temperature stabilization in the laboratory. Even though the AWG 1104 is not made for such comparisons the agreement was always well below 100 μV/V and probably could also be improved by a better temperature stabilization.

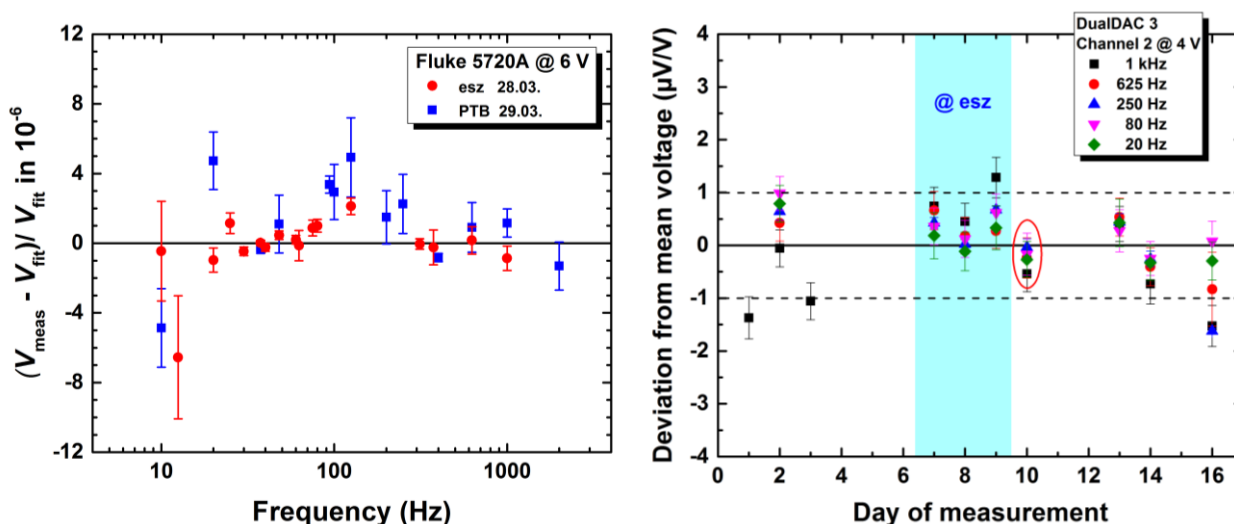


Fig. 17: Left Graph - Comparison of two AC quantum voltmeter at esz and PTB by using a Fluke 5720A calibrator at 6 V for the frequency range 10 Hz to 2 kHz. Right Graph - time trace for the Aivon Oy synthesizer output at 4 V and frequencies 20 Hz, 80 Hz, 250 Hz, 625 Hz and 1 kHz. The blue area shows the calibrations made at esz AG in Eichenau.

In summary, Objective 3 has been met in most cases. Especially, very good progress has been made with impedance matching approaches. Furthermore, calibration of commercial instruments against quantum standards went very well. This task has led to collaboration with manufactures of precision instrumentation. Further collaboration projects have already been arranged.

To demonstrated target uncertainties at 10 nV/V-level for frequencies up to 1 kHz and better than 10 μV/V up to 1 MHz. became difficult due to limited voltage amplitudes of only 2 mV_{p-p}. Nevertheless, proof-of-principle have been performed. To increase the voltage is just a technical task. It is expected that once a voltage at the volt-level is reached uncertainties in the range 10 nV/V are possible.

4.4 Objective 4

4.4.1 Voltage waveform scaling

In order to fully take advantage of new developments in Josephson voltage waveform measurement techniques, we need very high-quality voltage scaling devices for voltage levels higher than those that can be generated by Josephson voltage standards. These scaling devices should be broadband, linear, insensitive to the environment, and have small phase shifts. For this purpose, a new design of resistive voltage divider was constructed for 1 kV and 100 V input voltages. Here the new designs and the results of the characterization of the dividers are given.

The goal of the new design was to improve the level dependence at AC, to improve the frequency response and to reduce the sensitivity to air humidity compared to the previous generation of dividers at RISE. We also wanted to improve the safety of the design, since the previous dividers had a metal case which could get a high voltage if the divider was connected the wrong way. Fig.18. illustrates the design principle. Two adjustable screens surround the high voltage arm, connected to the input voltage and common low respectively. The screens are adjusted until the frequency response is flat. An external capacitive load and a buffer amplifier are connected to the output, and the capacitance is adjusted to make the phase response as low as possible.

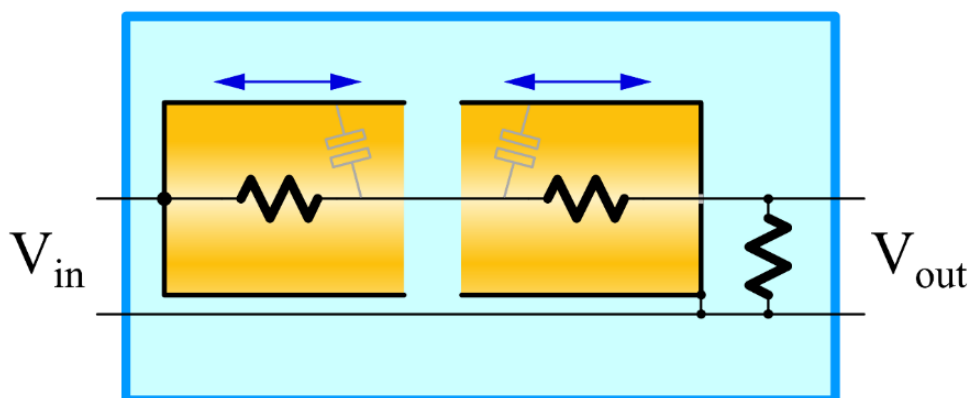


Fig. 18: Schematic principle of the voltage divider design. Two screens are surrounding the two resistors in the high voltage arm, one is connected to the input voltage, the other to the common low potential. The screens are movable in order to adjust the stray capacitance. When the capacitive leakage currents to the screens are in balance, the frequency response is flat.

In order to eliminate the sensitivity to air humidity we chose hermetically sealed resistors in both the high and low voltage arm. These resistors also have very low temperature and power coefficients. Also, to decrease the power dissipation the resistance in the divider has been increased by a factor of two compared to our earlier design. We constructed a plastic case for the printed circuit board to protect against electric shock. We tested two different circuit board materials, standard FR4 and a low loss laminate RO4003C, but could not measure any significant difference in performance. Fig.19. shows one of the prototype dividers.

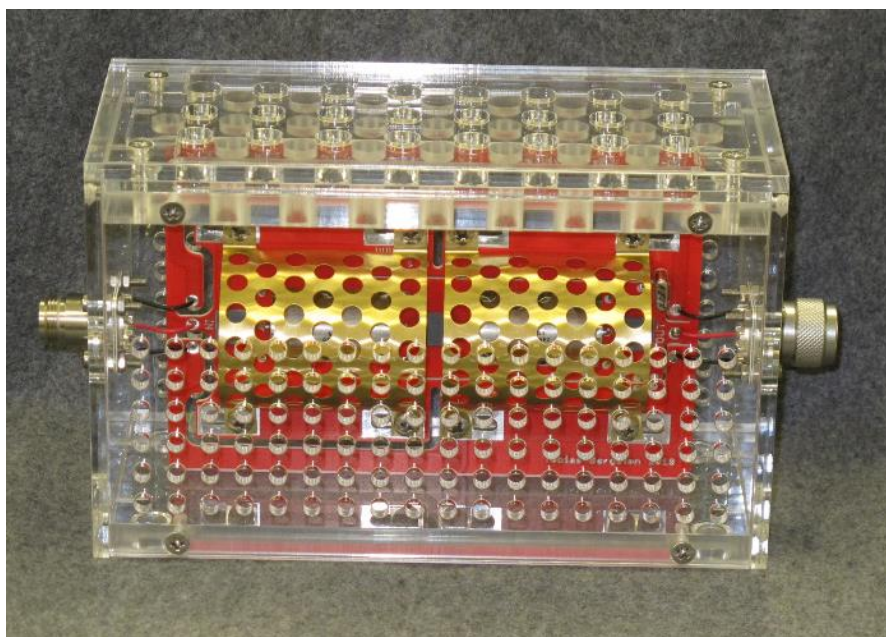


Fig. 19. One of the finished prototype dividers for 1 kV mounted in the plastic case.

4.4.2 New precision buffer amplifier

A new precision buffer amplifier with low input capacitance has been developed by CMI. Measurements showed a flatness below $0.1 \mu\text{V/V}$ up to 10 kHz, $2 \mu\text{V/V}$ at 100 kHz, and below $100 \mu\text{V/V}$ at 1 MHz. The input capacitance is below 1 pF, and the output impedance below $150 \text{ m}\Omega$ at 1 MHz. This buffer amplifier, as shown in Fig. 20, was very valuable for the project and has been used by many partners to evaluate the dividers. Detailed information of the divider has been published as open access. At CEM, the buffer was tested alone versus two Thermal Voltage Converters (TVC's), showing the possibility of using it not only in combination with a resistive divider but with Multijunction Thermal Converters (MJTC's), the most accurate type of TVC's in measuring situations where their use was not previously possible due to their low input impedance. Such situations could include the calibration of MJTC's versus an AC Josephson Voltage Standard both the type PJVS or JAWS, or the calibration of the ac-dc difference of a divider or high value resistor against the MJTC.



Fig. 20: Picture of the new precision buffer amplifier.

4.4.3 Characterization of the RISE divider

The dividers have been characterized by measuring the ac-dc voltage transfer difference and the DC-ratio at RISE. From these results the ac-ratio can be determined. Before the characterization the phase angle displacement of the divider and buffer amplifier is optimized by adjusting the two screens and the capacitive load until the influence of the reactive part on the frequency flatness is small or negligible

4.4.4 AC voltage ratio of the 1 kV divider

The frequency flatness of a divider can be characterized by measuring its AC-DC voltage transfer difference which corresponds to the relative correction needed to get an ideal frequency flatness. To minimize the influence of loading errors the resistive voltage divider was combined with a buffer amplifier on the output. The AC-DC differences of the input and output voltages of the voltage divider and buffer amplifier was measured by thermal voltage converters (TVCs) in an ac-dc transfer measuring system. Correction is

made for the ac-dc voltage difference of the two TVCs. The measured results for the 1000 V resistive voltage divider (S/N VDX-1902) and buffer amplifier is given in Table 1 and the expanded uncertainties are given in Table 2.

Table 1: The measured ac-dc difference of the new resistive voltage divider + buffer amplifier with ratio 1000 V to 0.8 V and its level dependence.

Divider range	S/N	Input voltage /V	Ac-dc voltage difference in $\mu\text{V}/\text{V}$ at frequency in Hz								
			10	20	45	110	1 k	10 k	20 k	50 k	100 k
1000 V	VDX-1902	1000	2.5	0.5	0.6	0.3	-0.6	-3.0	6.8	76	253
1000 V		500	3.9	0.7	1.1	0.3	-0.4	-3.6	-3.9	-20	-146
Level depend		1000 -> 500	1.4	0.2	0.5	0.0	0.2	-0.6	-10.7	-96	-399

Table 2: Expanded uncertainty of the measured ac-dc difference of the new resistive voltage divider + buffer amplifier with ratio 1000 V to 0.8 V.

Divider range	S/N	Input voltage /V	Expanded uncertainty in $\mu\text{V}/\text{V}$ at frequency in Hz								
			10	20	45	110	1 k	10 k	20 k	50 k	100 k
1000 V	VDX-1902	1000	6.8	6.2	6.0	6.0	5.7	6.9	8.0	14	26
1000 V		500	6.3	5.7	5.3	5.3	5.2	6.0	6.4	9	15
Level depend		1000 -> 500	4.3	3.3	3.0	3.0	2.9	3.4	4.9	11	22

The new design of the 1000 V divider + buffer amplifier gives good results to 10 kHz. From 20 Hz to 1 kHz the ac-dc differences are $\leq 1 \mu\text{V}/\text{V}$ at 1000 V with an expanded uncertainty of $6 \mu\text{V}/\text{V}$. Above 10 kHz the ac-dc difference shows a level dependence, $-399 \mu\text{V}/\text{V}$ at 100 kHz, when the voltage changes from 1000 V to 500 V. The reason for the level dependence will need more investigation, the PCB cause a minor part, but the major part is most likely due to leakage in the resistors.

4.4.5DC voltage ratio

The DC voltage ratio was measured on the resistive voltage divider only as the buffer amplifier used in the ac-dc transfer measurements have some drift in the dc-offset, within $\pm 10 \mu\text{V}$.

The dc voltage ratio of the resistive voltage divider ratio 1000 V to 0.8 V was calibrated by measuring the input and output voltage by digital voltmeters. The ratio is measured with input voltage 1000 V and 500 V and to minimize the influence of thermal emfs both positive and negative polarity are applied. The DC-ratios given in Table 3 below are measured after 30 minutes warm up.

Table 3: Measured DC voltage ratio and expanded uncertainty of the new resistive voltage divider only.

Divider range	S/N	Input voltage /V	Nom ratio	Measured DC-ratio	Relative correction / 10^{-6}	Expanded uncertainty / 10^{-6}
1000 V	VDX-1902	1000	1250	1249.979	-17.1	1.8
1000 V		500	1250	1249.982	-14.2	1.6
Level depend		1000 -> 500			2.9	1.6

The level dependence is $< 3 \mu\text{V}/\text{V}$. Fig. 21 shows the behavior of the voltage divider during warm-up when 1000 V is applied and cool-down when changing to 500 V. The step changes are the effect of the thermal emfs

when the polarity is reversed. Although the influence on the output voltage due to thermal emfs vary from $2 \mu\text{V/V}$ to $5 \mu\text{V/V}$ the measured ratio repeats within a few tenths of a $\mu\text{V/V}$. The drift of the DC ratio from 10 min to 30 min is $<0.5 \mu\text{V/V}$.

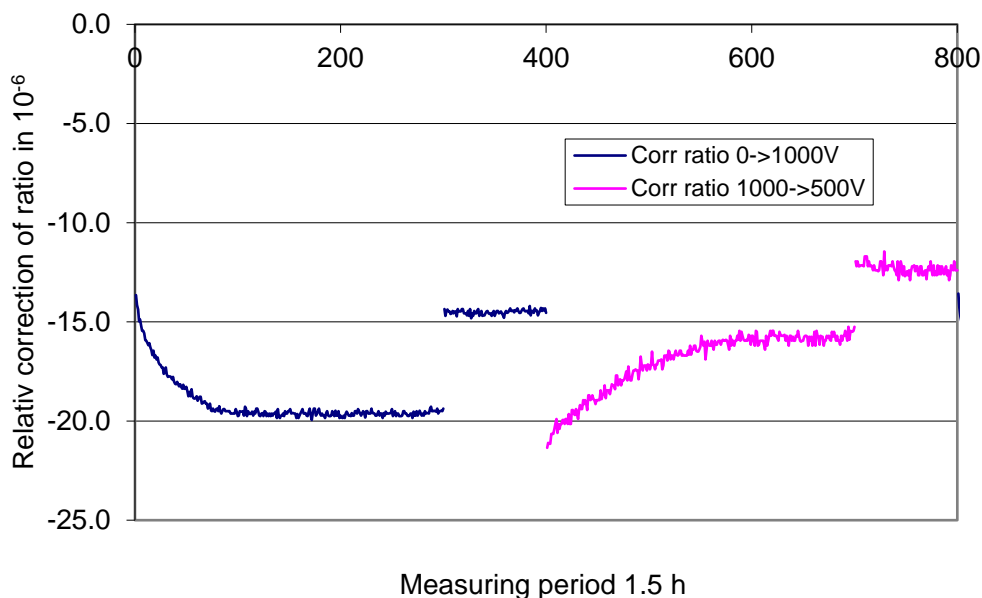


Fig. 21: Calibration of the dc voltage ratio of the resistive voltage divider ratio 1000 V to 0.8 V. The graph shows a measurement of the relative correction of the ratio relative to time (number of measurements). The first part is during warm up when +1000 V is applied, and next part is when -1000 V applied (blue). Then during cool down when +500 V is applied and finally when -500 V is applied (pink).

4.4.6 AC voltage ratio of the 1 kV divider

The AC voltage ratio of the new 1 kV resistive voltage divider together with a buffer amplifier is characterized at 1000 V from 20 Hz to 1 kHz with an expanded uncertainty of $6.5 \mu\text{V/V}$, which is close to the target uncertainty $5 \mu\text{V/V}$ at 50 Hz.

4.4.7 AC voltage ratio of 100 V divider

The 100 V divider was characterized in a similar way as the 1 kV divider. The ac voltage ratio of the new 100 V resistive voltage divider together with a buffer amplifier is characterized at 100 V up to 100 kHz with an expanded uncertainty of $6.7 \mu\text{V/V}$, which is well within the target uncertainty $25 \mu\text{V/V}$ at 100 kHz.

VSL, CEM and PTB have also made measurements to characterize the 100 V divider together with the buffer amplifier for frequencies up to 100 kHz. In most cases very similar results, as given by RISE have been achieved within the measurement uncertainties. In a few cases some unexpected behavior has been observed by CEM which will help to improve the devices and characterization routines in the future.

4.4.8 Divider design -TUBITAK

To construct ratio devices which have small level dependence, small time stability, small dependence against environmental conditions, and which can be calibrated with small calibration uncertainty two different ideas are explored by TÜBİTAK:

One of them is to construct a new resistive divider consisting of resistive guard and equal impedances as seen in Fig. 22. This design gives the opportunity to investigate different calibration techniques.

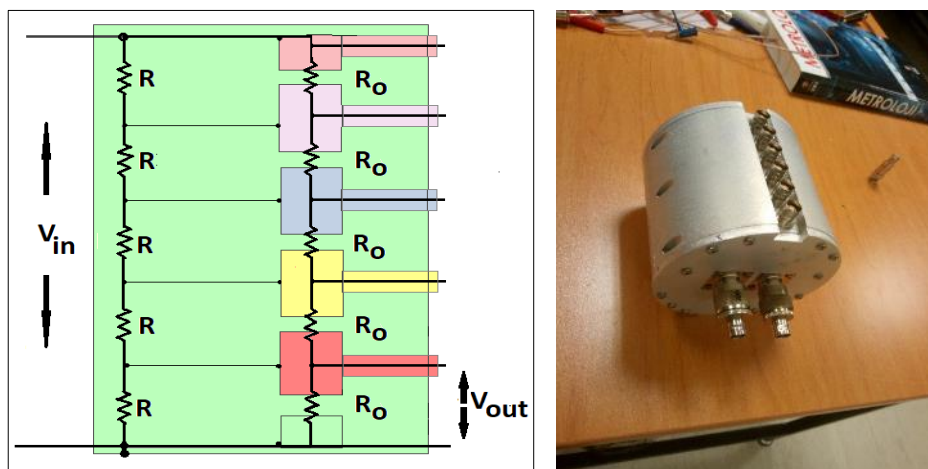


Fig. 22: Divider architecture and 5:1 Divider developed at TÜBİTAK.

Two dividers, one prototype with 5:1 ratio and one final version with 10:1 ratio, were manufactured in this manner. Established and commonly used AC-DC calibration methods for wideband resistive voltage dividers, have been used to investigate the ac level dependence, temperature, humidity and time stability effects for the new dividers. Humidity and temperature effects are negligible up to 10 kHz frequencies (see Fig. 23.). Also, the AC-DC difference up to 10 kHz and ac level dependence is small for the both dividers. The measurement results show a maximum ratio change of 6 $\mu\text{V/V}$ for temperature change and a maximum of 16 $\mu\text{V/V}$ due to a humidity change at 100 kHz. With these uncertainties for environmental influence and combining them with the calibration uncertainties the total uncertainty is still less than 25 $\mu\text{V/V}$. New calibration techniques to lower the calibration uncertainties of the dividers are still on-going. It is planned to report the results in a publication. The other idea is combining current shunts with range resistors which has small AC-DC difference at 100 kHz. Measurements are still being conducted to investigate level dependence and stability of such a divider.

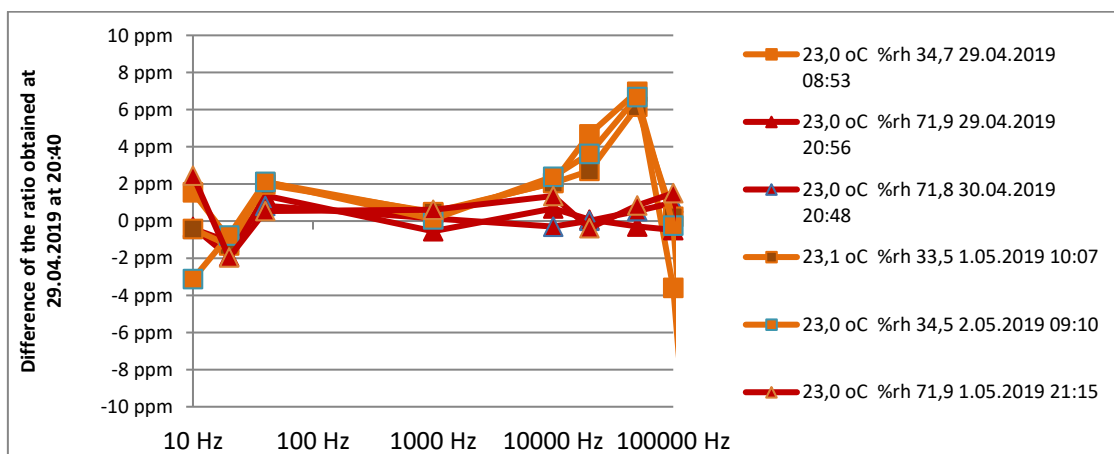


Fig. 23: Humidity dependence of TÜBİTAK's divider for a 10:1 ratio.

Finally, new broadband resistive voltage dividers with buffer amplifiers were developed by the project, to scale voltages down from 1 kV to 1 V, in a frequency range from DC to 1 MHz, with uncertainties of 6.5 $\mu\text{V/V}$ for 1 kV / 50 Hz and better than 25 $\mu\text{V/V}$ for 120 V / 100 kHz. A novel buffer amplifier developed and built by CMI already achieved perfect specifications. Voltage scaling is important for making AC quantum standards appropriate as replacements for current RMS AC methods. A new verification method based on pulse-driven Josephson arrays has been established at 10 nV/V level. Objective 4 has been achieved very well.

5. Impact

The partners have presented the project's achievements and progress at 13 different conferences. 13 publications have been submitted to peer-reviewed journals, 11 of which have been published already. During the project, there was regular interaction with standards organisations such as IEEE, DKD, EURAMET and training activities within the consortium have been carried out throughout the course of the project. A market survey of manufacturers/test companies on their requirements and the benefits of this EMPIR project was carried out by SC. Furthermore, an ADC workshop organized by NPL and SC and a dissemination meeting were held at NPL in Teddington, UK, on 16th January 2019 and 20-22 May 2019, respectively. As result of the work discussed in ADC workshop, CERN have expressed interest in the capability of the consortium to measure sub-Hz signals with a JJA based system to evaluate newly developed ADCs.

Impact on industrial and other user communities

This project will enable a step change in the delivery of traceability for time-varying quantities realised through electrical sensors. In particular, traceability for sampled electrical measurements, the basis of all modern instrumentation, will be provided to industrial end-users. As a first step, the consortium are working on utilising the quantum voltage digitiser as a new primary standard, opening more measurement capabilities of direct relevance to industrial communities. European instrumentation manufacturers attended project meetings for a discussion on calibrating test devices against the quantum voltage digitiser. In this way, they were directly involved in developing the measurement methodology for calibrating devices with this system and therefore were able to influence the future European quantum AC voltage calibration capabilities. Newly developed wideband scaling devices with optimum performance facilitate high voltages up to 1 kV and are directly linked to quantum standards. This development leads to improved methods for measuring and tracing power quality. In addition, there is a potential for commercial scaling devices to be built based on the knowledge gained during the project on developing prototypes.

To facilitate further uptake of the project's outputs there was considerable engagement throughout the project with industrial stakeholders including manufacturers of AC voltage measuring devices as well as other end-users and calibration laboratories. To ensure that the project was aligned with industrial needs a number of industrial partners participated in the project furthermore, a Stakeholder Committee was established. Three QuADC Newsletters have been distributed to inform interested stakeholders and parties about ongoing progress.

An international dissemination meeting with 50 participants from all over the world (20-22 May 2019) as well as seminars at the national level were organized. Furthermore, an ADC workshop has been held at NPL on 16th January 2019. This workshop and seminars were held to share project outputs and engage with the target end-user communities. Uptake of the new measurement capabilities developed by the project is expected as it will enable end-users to confidently demonstrate the performance of their products. In particular, uptake is expected amongst accredited laboratories and the manufacturers of ADC and spectrum analysers etc. and manufacturers of instrumentation relying on AC voltage measurements such as electrical power and power quality, and audio instrumentation.

A market survey of manufacturers / test companies on their requirements and the benefits of this EMPIR project has been carried out. A company and a big research institute have been attracted by promising results of the project.

Impact on the metrology and scientific communities

Conference presentations of project results e.g. including 7 at CPEM 2018, 8-13 July, Paris, France have been held at many international conferences. Furthermore, collaboration agreements have been signed by the consortium with one NMI and one company. Such agreements enhanced the working range of the project and, especially drew more worldwide attention from the quantum standards community so that the results of the project directly impacted the electrical quantum standards community, which is mainly formed by NMIs and high-level calibration laboratories. This community will be able to develop new measurement capacities based on the project's quantum standards. AC quantum voltage standards affect around 70 % of NMIs' calibration activity. As soon as targeted outcomes of this project such as 10 nV/V uncertainties for AC voltages are achieved they will contribute greatly to the future improvement of the European CMCs. The project had and will continue to have an impact in the electrical low-frequency community e.g. end-users involved in electrical sampling measurements and in dynamic quantities. The testing of commercial devices has been successfully executed within this project. Feedback to producers has raised their interest in further investigations as

quantum standards can give them a deeper insight in e.g. amplitude stability than any other conventional standard. These successful test calibrations already demonstrate how these instruments can be used in the metrology and scientific communities to provide easily traceability for AC voltages at the $\mu\text{V}/\text{V}$ -level. Hence, companies are being encouraged to improve their instruments such that they can enhance their position in the market. Furthermore, an application for a patent for a low-cost commercial pattern generator has been submitted. Such a generator will help to make the final quantum system compact and more affordable.

Impact on relevant standards

Results of the project have been reported to the Consultative Committee for Electricity and Magnetism (CCEM) and EURAMET Technical Committee for Electricity and Magnetism (TC-EM). This will support the metrological activities of key international and European committees. Furthermore, a presentation on project activities was given at standards organisations such as the Institute of Electrical and Electronics Engineers (IEEE) TC10 Waveform generation, measurement and analysis committee. IEC TC 85 Measuring equipment for electrical and electromagnetic quantities and IC TC 100 Audio, video and multimedia systems and equipment have been informed about the activities and the calibration methods developed in the project. Industrial committees like Verein Deutscher Ingenieure (VDI), Calibration of electrical quantities and DC and LF Metrology of the German calibration service (DKD) have also been informed about project activities. These participations build on activities already established by members of the consortium, who are highly influential in national and international metrology and standards committees and will be used to facilitate greater awareness of the project results.

Longer-term economic, social and environmental impacts

The project will enhance the metrology for electrical voltage and other time-varying quantities by means of new techniques for the application of precision measurements. Calibration laboratories, other stakeholders, and industry will then profit by improved measurement capabilities in the next step. The world's new method can provide low logistical effort and downtime thanks to direct traceability to fundamental constants. In the long-term competitiveness of European calibration laboratories will be sustainably increased as a need for re-calibration can be limited to a minimum or even eliminated.

Direct scaling of the Josephson defined waveforms to higher voltages will enable improved traceability of power quality measurements which will lead to an efficiency improvement in European power grids. Lower losses will generate e.g. less CO₂ emission.

With the electrical instrument suppliers being the backbone of major advances in electronics and sensing equipment, the outcome of this project could have a vast impact on our society, economy, environment and even health. Advances in sensing technology by increasing performance, functionality and energy-efficiency of electronic devices could enable e.g. car companies to enhance their capability of building autonomous driving cars.

6. List of publications

Dongsheng Zhao, Helko E van den Brom and Ernest Houtzager, "Mitigating voltage lead errors of an AC Josephson voltage standard by impedance matching," *Meas. Science and Technol.* 28 (2017) 095004.
<https://doi.org/10.1088/1361-6501/aa7aba>, <https://zenodo.org/record/3265687#.XWZU5OhKgdU>

Eivind Bardalen, Helge Malmbekk, Muhammad Nadeem Akram and Per Ohlckers, "Reliability study of fiber-coupled photodiode module for operation at 4 K," *Microelectronics Reliability Journal*, November 11, 2017.
<https://doi.org/10.1016/j.microrel.2017.10.034>

Andrea Sosso and Paolo Durandetto, "Experimental analysis of the thermal behavior of a GM cryocooler based on linear system theory," *International Journal of Refrigeration*, Vol. 92, August 2018, pp. 125-132.
<https://doi.org/10.1016/j.ijrefrig.2018.04.016>

Bjørnar Karlsen, Oliver Kieler, Ralf Behr, Thai Anh Tuan Nguyen, Helge Malmbekk, Muhammad Nadeem Akram, and Per Ohlckers, "Pulsation of InGaAs photodiodes in liquid helium for driving Josephson arrays in ac voltage realization," *IEEE Trans. Appl. Supercond.*, Vol. 29, No. 7, Oct. 2019, 1200308.
<https://doi.org/10.1109/TASC.2019.2901573>

Oliver Kieler, Bjørnar Karlsen, Per Alfred Ohlckers, Eivind Bardalen, Muhammad Nadeem Akram, Ralf Behr, Jane Ireland, Jonathan Williams, Helge Malmbekk, Luis Palafox, and Ruediger Wendisch, "Optical pulse-drive for the pulse-driven AC Josephson voltage standard," IEEE Trans. Appl. Supercond., Vol. 29, No. 5, Aug. 2019, 1200205.

<https://doi.org/10.1109/TIM.2018.2877562>

J. Ireland, J. Williams, O. Kieler, R. Behr, E. Houtzager, R. Hornecker, H.E. van den Brom, "An Optoelectronic Pulse Drive for Quantum Voltage Synthesizer", vol. 68, no. 6, pp. 2066-2071, June 2019.

<https://doi.org/10.1109/TIM.2018.2877562>

Allan Belcher, Jonathan Williams, Jane Ireland, Ricardo Iuzzolino, Marcos E. Bierzychudek, Ronald Dekker, Jonas Herick, Ralf Behr and Kars Schaapman, "Towards a Metrology class ADC based on Josephson junction devices", Journal of Physics, Conference Series: 1065 052044.

<https://doi.org/10.1088/1742-6596/1065/5/052044>

Eivind Bardalen, Bjørnar Karlsen, Helge Malmbekk, Muhammed Nadeem Akram, Per Ohlckers, "Evaluation of InGaAs/InP photodiode for high-speed operation at 4 K", EDP Sciences, Int. J. Metrol. Qual. Eng. 9, 13 (2018).

<https://doi.org/10.1051/ijmqe/2018015>

Eivind Bardalen, "Reliable Packaging and Development of Photodiode Module for Operation at 4 K", Doctoral dissertations at the University of South-Eastern Norway no. 5.

<http://hdl.handle.net/11250/2500465>

7. Contact details

Coordinator	Ralf Behr	PTB	Tel: +49 531 592 2630	E-mail: ralf.behr@ptb.de
WP1 leader	Jane Ireland	NPL	Tel: +44 20 8943 6099	E-mail: jane.ireland@npl.co.uk
WP2 leader	Helge Malmbekk	JV	Tel: +47 64848427	E-mail: hma@justervesenet.no
WP3 leader	Helko van den Brom	VSL	Tel: +31 15 269 1726	E-mail: hvdbrom@nmi.nl
WP4 leader	Jonas Herick	PTB	Tel. +49 531 592 2135	E-mail: jonas.herick@ptb.de
WP5 leader	Félix Raso Alonso	CEM	Tel: +34 91 807 48 26	E-mail: fraso@cem.mityc.es